Pergamon

J. Appl. Maths Mechs, Vol. 61, No. 2, pp. 333–337, 1997

PII: S0021-8928(97)00042-7
0021-8928/97 \$24.00+0.00

SECONDARY BRANCHING AND THE POST-CRITICAL BEHAVIOUR OF THIN-WALLED SHELLS DURING NON-UNIFORM DEFORMATION†

I. P. ZHELEZKO and N. I. OBODAN

Dnepropetrovsk

(*Received* 10 *January* 1996)

The non-linear behaviour and post-critical behaviour of thin-walled shells during non-uniform deformation due to a non-uniform load or inhomogeneous structure are analysed. The branching equations are constructed and, for the non-linear equations for Newton's method, the singular points are classified. The results of calculations and an analysis of the post-critical behaviour for cylindrical and spherical shells with inhomogeneities of different forms are given. It is shown that localized patterns of stability loss and fracture are due to the existence of isolated equilibrium branches and secondary branching of non-linear solutions.

It has been established in experimental investigations [1] that the post-critical equilibrium shapes of thin shells can be subdivided into general (regular) and local shapes, wave formation in the latter being expressed on only a bounded part of the surface. The boundary of the region of existence of local post-critical shapes is below that of regular states. The true carrying capacity of a buckled structure can be estimated by investigating post-critical states of thin-walled structures in non-uniform deformation. Previous theoretical analyses of the post-critical behaviour of thin-walled structures mainly concern the initial segments of post-critical branches, the buckle patterns being taken as the characteristic linear shapes of the bifurcation problem for a homogeneous subcritical state [2]. In the case of similar critical loads corresponding to different linear buckling patterns, it has been shown that interaction between adjacent shapes might manifest itself in secondary bifurcation of post-critical branches [3]. We have obtained solutions of this kind for a model with two degrees of freedom, corresponding to two adjacent linear shapes. We have not made a full non-linear analysis of secondary branching. We have restricted the investigation of local buckling to the analysis of an example of the formation of a single dent of given shape at loads close to the classical critical value.

1. STATEMENT OF THE PROBLEM AND NUMERICAL METHOD

We consider a geometrically non-linear boundary-value problem of the theory of shells in non-uniform deformation. The square of the angles of rotation during deformation is assumed to be not greater than one. The corresponding variational problem involves finding the minimum of the functional

$$S=-\frac{1}{2Eh}\iint\left[\left(T_{11}^2+T_{22}^2-2\nu T_{11}T_{22}+\frac{2}{1+\nu}T_{12}^2\right)+\frac{12}{h^2}\left(M_{11}^2+M_{22}^2-2\nu M_{11}M_{22}+\frac{1}{1+\nu}M_{12}^2\right)\right]d\Omega+$$
$$+\iint\left\{T_{11}\frac{1}{A_1A_2}\left[A_2\frac{\partial u}{\partial\xi}+\frac{\partial A_1}{\partial\eta}v+A_1A_2\frac{w}{R_1}+\frac{1}{2}A_1A_2\vartheta_1^2\right]+\right.$$
$$+T_{22}\frac{1}{A_1A_2}\left[A_1\frac{\partial v}{\partial\eta}+\frac{\partial A_2}{\partial\xi}u+A_1A_2\frac{w}{R_2}+\frac{1}{2}A_1A_2\vartheta_2^2\right]+$$
$$+T_{12}\frac{1}{2A_1A_2}\left[A_2\frac{\partial v}{\partial\xi}+A_1\frac{\partial u}{\partial\eta}-\frac{\partial A_2}{\partial\xi}v-\frac{\partial A_1}{\partial\eta}u+A_1A_2\vartheta_2\vartheta_1\right]+$$
$$+M_{11}\frac{1}{A_1A_2}\left[A_2\frac{\partial\vartheta_1}{\partial\xi}+\frac{\partial A_1}{\partial\eta}\vartheta_2\right]+M_{22}\frac{1}{A_1A_2}\left[A_1\frac{\partial\vartheta_2}{\partial\eta}+\frac{\partial A_2}{\partial\xi}\vartheta_1\right]+$$
$$\left.+M_{12}\frac{1}{2A_1A_2}\left[A_2\frac{\partial\vartheta_2}{\partial\xi}+A_1\frac{\partial\vartheta_1}{\partial\eta}-\frac{\partial A_2}{\partial\xi}\vartheta_2-\frac{\partial A_1}{\partial\eta}\vartheta_1\right]\right\}d\Omega+\lambda\iint q\,d\Omega \tag{1.1}$$
$$\vartheta_1=\frac{1}{A_1}\frac{\partial w}{\partial\xi}+\frac{1}{R_1}u,\quad \vartheta_2=\frac{1}{A_2}\frac{\partial w}{\partial\eta}+\frac{1}{R_2}v$$

†*Prikl. Mat. Mekh.* Vol. 61, No. 2, pp. 344–349, 1997.

The integration is carried out over the entire surface of the shell, ξ and η are the coordinate axes, λ is the load parameter, R_1 and R_2 are the radii of curvature of the undeformed surface in directions ξ, η, A_1 and A_2 are the Lamé parameters of the median surface, h is the shell thickness, E is Young's modulus and D is Poisson's ratio.

Notice that all the resolvents of the theory of shells—the equations of consistency, elasticity and equilibrium, as well as the natural boundary conditions—follow from the conditions for functional (1.1) to be stationary.

The components of the vector $\mathbf{U} = \{u, v, w, T, M\}$ can be represented in the form

$$U_i(\xi,\eta)=\sum_{r=1}^{4} U^i_{2j+r}H_r(\xi)$$

$$U^i_{2j+r}(\eta)=\begin{cases}\mathbf{U}^i(\xi_j,\eta), & r=1,3\\ \dfrac{\partial \mathbf{U}^i}{\partial\xi}(\xi_j,\eta), & r=2,4\end{cases} \tag{1.2}$$

where ξ_j is the coordinate of the jth node on the shell generator from which the directrix emerges.

The coordinate functions $H_r(\xi)$ are taken as Hermite polynomials.

Applying the Kantorovich procedure to functional (1.1), we can write the resolvent system of equations for functions $U_k(\eta)$ in the form

$$F(U^i_{2j+r},\eta,\lambda)=0,\quad r=1,\ldots,4;\quad i=1,\ldots,5 \tag{1.3}$$

with conditions on the boundaries $\eta = \eta_1, \eta_2$

$$\mathbf{G}(\mathbf{A})=0,\quad \mathbf{A}=\{U^i_k(\eta)\} \tag{1.4}$$

For a known value of the vector $\mathbf{A}$, the system of ordinary differential equations (1.3) can be integrated numerically by reducing boundary-value problem (1.3), (1.4) to a Cauchy problem. Thus, if conditions (1.3) are satisfied in advance, the solution of the problem of a minimum of functional (1.1) will reduce to determining $\mathbf{A}$, by Newton's method for example

$$\mathbf{A}^{(k+1)}=\mathbf{A}^{(k)}-\mathbf{G}_A^{-1}\mathbf{G}(\mathbf{A}^{(k)}) \tag{1.5}$$

$$\mathbf{G}_A=\{\partial G_i/\partial A_j\},\quad i,j=1,2,\ldots,n$$

where $\mathbf{A}^{(k)}$ is the kth approximation to the solution, $\mathbf{G}_A$ is the Jacobian, and n is the order of the resolvent. If conditions (1.3) are satisfied in advance, the branching condition of the boundary-value problem corresponding to variational problem (1.1) has the form

$$\det\mathbf{G}_A=0 \tag{1.6}$$

What type of branch point it is (a limit point or bifurcation point) is determined by equating to zero the minors of the matrix $\mathbf{G}_\lambda$ obtained from the Jacobian $\mathbf{G}_A$, augmented by the column $\partial\mathbf{G}/\partial\lambda$.

When $\det\mathbf{G}_A = 0$, rank $G_\lambda = n$, it is a bifurcation point; when $\det\mathbf{G}_A = 0$, $\det B_{\lambda n} \neq 0$, where $\mathbf{B}_{\lambda n}$ is any minor of order n of the matrix $\mathbf{G}_\lambda$, it is a limit point.

Thus, algorithm (1.5) can be used to find and classify the branching points and solve problem (1.1) at the same time.

2. NUMERICAL CONSTRUCTION OF THE BRANCHING EQUATION

In cases where the singular point is a limit point, the post-critical branch of the solution can be constructed by changing the independent parameter for continuing the solution. However, if the singular point is a bifurcation point, the branching equation must be obtained before the post-critical branch can be constructed [4]. Assuming that the condition $G(\mathbf{A}^\circ, \lambda^\circ) = 0$ is satisfied, the solution $(\mathbf{A}^\circ, \lambda^\circ)$ is known, and the solution $(\mathbf{A}^\circ + \tilde{\mathbf{A}}, \lambda^\circ + \tilde{\lambda})$ corresponds to the post-critical point, if the rank of the matrix $\tilde{\mathbf{G}}(\mathbf{A}^\circ, \lambda^\circ\, \tilde{\mathbf{A}}, \tilde{\lambda})$ constructed for the solution $(\mathbf{A}^\circ + \tilde{\mathbf{A}}, \lambda^\circ + \tilde{\lambda})$ at branching point $(\mathbf{A}^\circ, \lambda^\circ)$ is equal to r and $\tilde{\mathbf{A}} = \{\tilde{\mathbf{A}}_1, \tilde{\mathbf{A}}_2\}$, where $\tilde{\mathbf{A}}_1$ is a vector of order r and $\tilde{\mathbf{A}}_2$ is a vector of order $n - r$, the branching equation has the form [4]

$$R(\tilde{\mathbf{A}}_2)=(\mathbf{B}_{21}\mathbf{B}_{11}^{-1}\mathbf{C}_1-\mathbf{C}_2)\tilde{\lambda}+\mathbf{Q}_1\mathbf{B}_{21}\mathbf{B}_{11}^{-1}-\mathbf{Q}_2=0 \tag{2.1}$$

for

$$\tilde{\mathbf{A}}_1 = \mathbf{B}_{11}^{-1}\mathbf{B}_{12}\tilde{\mathbf{A}}_2 + \mathbf{B}_{11}^{-1}\mathbf{C}_1\lambda + \mathbf{B}_{11}^{-1}\mathbf{Q}_1 \tag{2.2}$$

where $\mathbf{Q}_1$, $\mathbf{Q}_2$ are the highest terms of the series

$$\mathbf{C} = \{\mathbf{C}_1, \mathbf{C}_2\}^T = \frac{\partial \tilde{G}_i(A^\circ, \tilde{A}, \tilde{\lambda})}{\partial \tilde{\lambda}}, \quad \mathbf{B}_{ij} = \left(\frac{\partial \tilde{G}_i(A^\circ, \tilde{A}, \tilde{\lambda})}{\partial \tilde{A}_j}\right)$$

$\mathbf{B}_{11}$, $\mathbf{B}_{12}$ are the minors of matrix B of order r, and $\mathbf{B}_{21}$, $\mathbf{B}_{22}$ are the minors of B of order $n - r$.

Since the resulting equation does not contain linear terms in $\tilde{\mathbf{A}}_2$ [4], it does not have a unique solution for $\tilde{\mathbf{A}}_2$.

A solution starting from the bifurcation point is constructed numerically. The vector $\tilde{\mathbf{A}}_2$ is found from the branching equation by Newton's method. The vector $\tilde{\mathbf{A}}_2$ is used as the vector argument. The vector $\tilde{\mathbf{A}}_1$ is computed using formula (2.4), disregarding terms of the highest order of smallness. The vector $\tilde{\mathbf{A}}_2$ is determined by Newton's method from the system of equations (2.1)

$$\tilde{\mathbf{A}}_2^{(k+1)} = \tilde{\mathbf{A}}_2^{(k)} - \mathbf{P}^{-1} R(\tilde{\mathbf{A}}_2^{(k)}) \tag{2.3}$$

$$P_{ij} = \left\{\frac{\partial R_i(\tilde{\mathbf{A}}_2)}{\partial \tilde{A}_{2j}}\right\} \tilde{\mathbf{A}}_2 = \tilde{\mathbf{A}}_2^{(k)}$$

The increment of the load parameter is given a small fixed value.

The vector $\tilde{\mathbf{A}}_2$, determined with prescribed accuracy, and the vector $\tilde{\mathbf{A}}_1$, computed using formula (2.2), are used for the initial approximation to continue the solution along the post-critical branch using algorithm (1.5).

3. RESULTS

We used the algorithm to construct solutions of the problem for the advanced post-critical stage of the deformation of shells of different kinds and to determine how those solutions change, depending on the type of non-uniformity of the deformation.

Figure 1 shows the pattern of post-critical solutions for a cylindrical shell with axisymmetric applied pressure. Here W is the maximum deflection relative to shell thickness and λ is the load parameter relative to its critical value, determined from the linearized problem.

With a load $\lambda = 1$ on branch OA, corresponding to the initial axisymmetric state, we reach bifurcation point A. The branch $ABCD$ corresponds to the post-critical regular solution (deflection 1); the lower boundary of existence of the regular shape is $\lambda = 0.72$. The secondary branching point B is fixed on branch AD with a level of the amplitude of the deflection $W = 4$. The shell deflection pattern corresponding to the solution BE is very localized: the extent of localization—the depth of the dent—increases and the amplitude of the regular component decreases with distance from the bifurcation point B along BE. The lower boundary of the existence of a pattern of local equilibrium with one dent (deflection 2) corresponds to the load $\lambda = 0.53$.

There is another secondary branching point C with a localized branching solution, at the level of amplitudes of the regular solution $W = 8$, but in this case there is a group of dents which is symmetric about the two orthogonal meridional planes (deflection 3). The corresponding branch of the diagram is FCF and the lower critical load is $\lambda = 0.62$. Thus there is one zone in which only regular post-critical patterns form and one where localized buckling occurs, its lower boundaries lying below the lowest level of perturbed loads for a regular pattern. If the load has

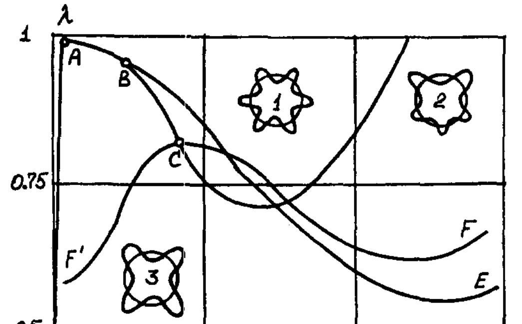

Fig. 1.

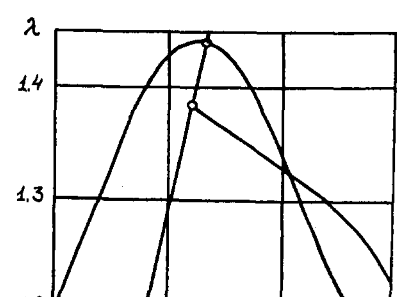

Fig. 2.

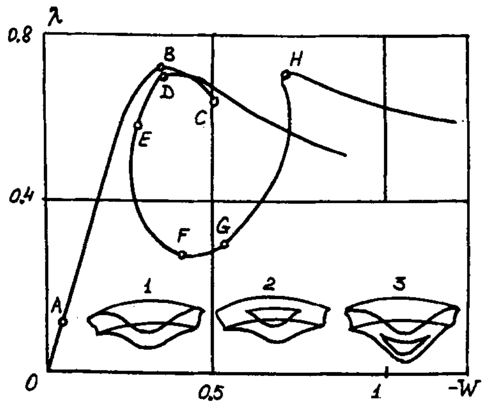

Fig. 3.

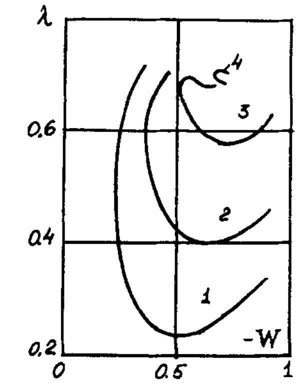

Fig. 4.

a non-axisymmetric component $q = (\lambda/2)(1 + \cos(n\eta))$, the pattern of post-critical deformation is partly destroyed—bifurcation point A becomes a limit point, and bifurcation points of type B and C move to the initial ascending branch (Fig. 2). For instance, in the case $n = 8$ the solution with a deflection with one local dent branches at the lowest bifurcation point of the post-critical regular solution $\lambda = 1.39$; the second critical load $\lambda = 1.42$ correspond to branching with a group of local dents. The curves $\lambda - W$ preserve their character and remain descending.

It should be emphasized that the solutions which describe local bending exist in the neighbourhood of regular deflectional solutions, whatever their nature—whether the pattern that develops is pre- or post-critical. The way in which the bifurcation pattern changes depends on the parameter p, equal to the ratio of variability of the regular solution of type 1 to that of the load function n. When $p > 1$, the branching pattern has the form shown in Fig. 2, when $p \leqslant 1$, the diagram splits into upper and lower branches, and the lower branch has a limit point.

The deformation pattern for spherical segments was previously observed to change with the geometric parameter ρ in a similar way [5].

The branching pattern becomes very much more complicated in the case of two-layer shells which separate on one part of the surface, where the layers might deform separately.

Thus, Fig. 3 shows the pattern of $\lambda - W$ for a two-layer spherical shell with a separated part. The point B here is both a limit point for the solution of type 1 and a bifurcation point for the solution of type 2. The curve has a limit point of its own, corresponding to general buckling of the shell with a localized buckled layer (deflection 3). The curve ABC corresponds to a process of deformation in which the layers maintain contact up to the maximum value $\lambda = 0.72$. The deflection is similar to post-critical deflections of a spherical segment of the same geometry without a separation zone. The critical load is also very nearly the same as that for a monolithic shell with the same geometry.

As the stratification parameters vary, there is a considerable change in the branch DEF, which describes the equilibrium states with a buckled layer. Thus, as the relative separation thickness h_1/h increases (h_1 is the thickness of the layers and h is the thickness of the packet), the branch of type DEF degenerates and disappears (Fig. 4) when $h_1/h = 0.24$.

The relative thickness at which a local loss of stability is impossible depends on the dimensions of the separation zone. The stable value of the limiting relative thickness at separation angles $\varphi_d = 0.09$ is associated with the presence of a resonance angle of shopping. As we have shown, for separation angles greater than this resonance angle φ_d, the values of the lower limiting loads and the shape of isolated curves do not change near those loads. For large φ_d, however, this resonance angle remains almost constant in value and, as Fig. 5 shows, $\varphi_{dr} = 0.09$ for $h_1/h = 0.25$. For the specified geometry with $\varphi_{dr} = 0.09$, the limiting relative thickness is not more than 0.24.

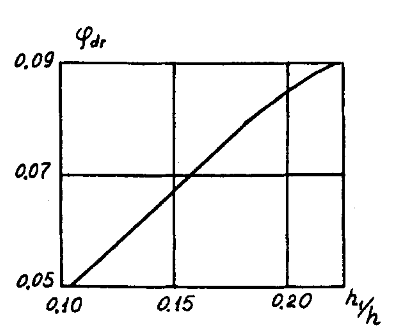

Fig. 5.

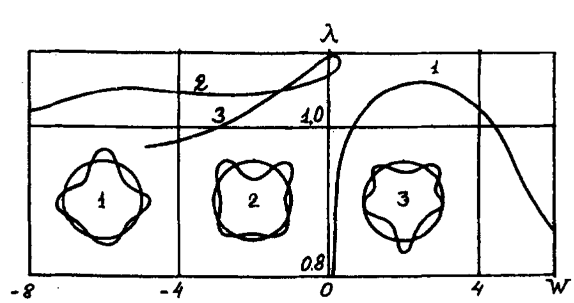

Fig. 6.

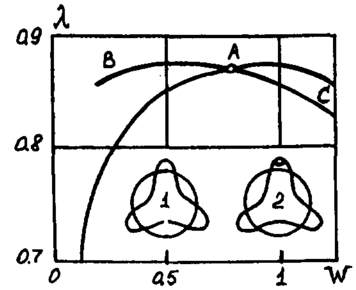

Fig. 7.

For a cylindrical shell with a rectangular separation zone exposed to a uniform applied pressure, there is a considerably narrower range of shapes with a buckled lower layer. This appears to be due to the lower level of compressive stresses and the fact that the ratio of the critical loads of the whole shell and of the panel corresponding to the separated part is different from that for a spherical shell.

Even in cases where no localized loss of stability has been discovered, separation destroys the branching pattern of Fig. 1. For a shell with $L/R = 4, R/h = 150, L/x_s = 10, R/y_s = 2.5, h_1/h = 0.1$ (x_s and y_s are the separation lengths in the longitudinal and transversal directions, respectively) the layers in the separation zone move parallel to one another, but the initial branch 1 (deflection 1) is joined by the isolated branch 2–3, where regular deflections of shapes 2 and 3, respectively, occur (Fig. 6). Lessening of stiffness leads to a reduction in the critical load on the initial branch to $\lambda = 0.84$.

The solutions in the buckled lower layer were obtained for a shell with $L/R = 6, R/h = 50, L/x_s = 5, h_1/h = 0.1$ (Fig. 7). In this case the initial branch with regular shape 1, for which the layers move together, have a branch point A with $\lambda = 0.92$ and deflection amplitude $W = 2.5$. For non-layered parts of the shell, the bending pattern of the shell corresponding to branch BAC (form 2) is similar to form 1, the local deflection of the buckled layer increasing as we move along BC.

REFERENCES

1. MOSSAKOVSKII, V. I., MANEVICH, L. I. and PROKOPALO, Ye. F., On post-critical patterns of equilibrium of cylindrical shells under applied pressure. *Dokl. Akad. Nauk SSSR*, 1975, **222**, 548–550.
2. HUTCHINSON, J. W. and KOITER, W. T., Postbuckling theory. *Appl. Mech. Rev.* 1970, **23**, 12, 1353–1366.
3. SUPPLE, W. J., On the change in buckle pattern in elastic structures. *Int. J. Mech. Sci.* 1968, **10**, 737–745.
4. VAINBERG, M. M. and TRENOGIN, V. A., *The Theory of Branching of the Solutions of Non-linear Equations*. Nauka, Moscow, 1969.
5. SRUBSHCHIK, L. S., *Buckling and Post-critical Behaviour of Shells*. Izv. Rost. Univ., Rostov, 1981.

Translated by R.L.